Carbon 149 (2019) 290–296

Contents lists available at ScienceDirect

Carbon

journal homepage: www.elsevier.com/locate/carbon

Early oxidation stages of germanium substrate in the graphene/Ge(001) system

P. Dabrowski [a, *], M. Rogala [a], I. Pasternak [b], P. Krukowski [a], J.M. Baranowski [c], W. Strupinski [b], I. Lutsyk [a], D.A. Kowalczyk [a], S. Pawłowski [a], Z. Klusek [a]

[a] Department of Solid States Physics, Faculty of Physics and Applied Informatics, University of Lodz, Pomorska 149/153, 90-236, Lodz, Poland
[b] Faculty of Physics, Warsaw University of Technology, Koszykowa 75, 00-662, Warsaw, Poland
[c] Institute of Electronic Materials Technology, Wolczynska 133, 01-919, Warsaw, Poland

ARTICLE INFO

Article history:
Received 14 December 2018
Received in revised form
30 March 2019
Accepted 8 April 2019
Available online 12 April 2019

ABSTRACT

Kelvin Probe Force Microscopy (KPFM) in combination with Atomic Force Microscopy (AFM), Scanning Tunneling Microscopy/Spectroscopy (STM/STS), and X-ray Photoelectron Spectroscopy (XPS) were used to study early stages of oxidation of germanium in the graphene/Ge(001) system exposed to atmospheric environment. KPFM measurements allowed to distinguish nanoscale regions, which are not covered by graphene, as a result of graphene domain misorientation in the growth process. In this area, corrosion process penetrated the region underneath graphene, which can be observed at the nano- and microscale. Therefore, the electronic properties of graphene/germanium hybrid system are modified in the regions around defects. Whereas graphene can protect surfaces against oxidation, the described processes have impact of electronic properties of the sample in a long time scale. We showed that early oxidation stages can be identified in nanoscale even when macroscopic techniques such as XPS do not show signs of degradation. The obtained results are important for assessing the need of protection of graphene/Ge(001) devices.

1. Introduction

Graphene layers can be obtained by different methods. Among others, there are mechanical exfoliation [1], reduction of graphene oxide [2] and chemical vapor deposition growth (CVD) on various substrates [3–5]. Particularly, CVD growth is the most promising fabrication method due to possibility of controlling quality and number of deposited graphene layers. Moreover, this method allows modification of electronic properties of the graphene layers during the growth process by intercalation [6,7] and by direct doping through substitution of carbon atoms [8,9]. The CVD growth is performed usually on the top of metal substrates such as Ni, Cu, Ir, Ru but also on the insulators like SiC [3,4]. Unfortunately, most of those substrates are not applicable in standard semiconducting technology. On the other hand, graphene removed from metals and transferred onto SiO_2 or h-BN substrates contains metal impurities [10,11]. In the case of SiO_2, there are also observed charge traps, which can modify significantly graphene electronic properties [12].

Those drawbacks can be overcome by the growth of graphene on single germanium crystal or dedicated Ge(001)/Si(001) substrate [13–22]. Recently, it has been shown that depending on the germanium face and growth conditions it is possible to obtain high-quality graphene layers [21] or even graphene nanoribbons [20]. It was also proposed that the growth of graphene on the top of Ge(001)/Si(001) substrate [15,19,23] is important to the potential compatibility with the metal oxide semiconductor technology (CMOS) [19]. This approach significantly reduces the cost of graphene production thanks to using only a 300 nm-thin layer of Ge. Similarly to graphene on other metal substrates, graphene grown on germanium can be transferred onto arbitrary substrates [16]. However, it should be emphasized that graphene transferred from germanium layer is free from metal impurities. This makes this system optimal for further applications and device manufacturing.

Another important issue is related to using graphene as a protective layer for substrates sensitive to atmospheric conditions [24–29]. The protection of substrate by graphene was extensively studied for graphene on top of copper foils and monocrystals. However, even for those well-defined and explored systems there

* Corresponding author.
E-mail address: pdabr@uni.lodz.pl (P. Dabrowski).

https://doi.org/10.1016/j.carbon.2019.04.036
0008-6223/

were contradicted findings presented in literature, which shows efficient protection [26] or even faster degradation [25]. Previously, we have found that the corrosion processes appeared in uncovered regions at the nanoscale and penetrated through graphene/copper interface [27], which is a crucial factor for many possible application of graphene/copper system. Graphene was described as an anticorrosion barrier also for germanium substrate [28]. The importance of those findings was related to lack of methods of the sufficient protection of germanium. Contrary to silicon systems, germanium oxides are unstable and therefore cannot protect germanium and limit its use in semiconducting industry [30,31]. There were also other methods of protection [30,32,33], but none of them give satisfactory results. At the same time, the recent research shows the possibility of germanium protections with graphene [28]. Germanium covered by graphene during growth shows no visible signs of corrosion after four months of the exposition for atmospheric condition [28]. It was additionally argued that graphene should be properly grown, as to receive the continuous protective layer on the germanium. However, in the case of multidomain grown there were always regions where defects in graphene layers will be presented. This is in the case of graphene grown on copper, where multidomain orientation is related with discontinuities in graphene layer due to different domain alignments [27] and due mechanism of grown [15]. Similar behavior should be considered for graphene on top of Ge(001) crystals.

The graphene growth on the top of Ge(001)/Si(001) substrate is complicated due to the existence of substrate nanofacets [23,34]. As a result, there are two main issues. Firstly, we obtain two different planar orientations of graphene domains. Secondly, we also acquire different domain alignments in the direction perpendicular to the surface [23]. Therefore, we expect that germanium surface is not entirely covered by graphene due to domains misalignment leading to the presence of exposed pure germanium patches. These patches can be susceptible to oxidation processes which may influence sample electronic properties significantly. Since germanium substrate is even more reactive than copper, and graphene has also different domain orientation on top of germanium substrate, we may expect similar phenomena for graphene/Ge samples. However, in the case of graphene growth on germanium the number of domain orientations is much smaller in comparison to the growth of graphene on copper foil. It should result in a lower density of defects. Due to the fact that graphene/Ge(001) systems might be potentially used in semiconductor industry, the studies of oxidation processes of germanium covered by graphene are critical and this issue deserves comprehensive investigations in large time scale. In this work, we show our x-ray photoelectron spectroscopy (XPS), Kelvin probe force microscopy (KPFM) together with scanning tunneling microscopy/spectroscopy (STM/STS) studies of early stages of oxidation of germanium substrate in the graphene/Ge(001)/Si(001) and graphene/Ge(001) systems both in ultra-high vacuum (UHV) and atmospheric environment. We have found that even when XPS was unable to detect early stages of oxidation, the presence of oxidized regions can be identified at the nanoscale. Moreover, we observed that the oxidation process expands under the graphene layer and on a longer time scale can cause significant degradation of graphene/germanium system. These studies help to answer the question whether graphene discontinuities allow oxidation processes which can propagate under the graphene layer like in the previously studied graphene on copper system. So far, this type of studies has not been reported in the literature.

2. Experimental

Graphene films were synthesized in a 6-inch Aixtron Black Magic system by CVD method as described in detail elsewhere [19]. As a substrate we used (001)-oriented Ge layers deposited on Si (001) wafers by CVD method and Ge(001) monocrystal. In manuscript we present results of most technologically relevant graphene/Ge(001)/Si(001) as we did not observe any significant differences between oxidation processes for this sample and graphene/Ge(001) monocrystals. Methane gas in the mixture of Ar and H_2 in the ratio of 20:1 was used as a carbon precursor. Prior to graphene growth, the substrate was annealed in pure hydrogen in order to in-situ reduce native oxides. All the measurements by STM, STS, current imaging tunneling spectroscopy (CITS), KPFM, and low energy electron diffraction (LEED) were carried out inside Multiprobe P (Scienta-Omicron) system in ultra-high vacuum (UHV) under the base pressure of 3×10^{-10} mbar. The KPFM measurements were conducted both in UHV using modulation detection mode (with the Matrix/Nanonis control system) and in ambient conditions using two-pass technique (with the NT-MDT Ntegra Aura system). Additionally, the local conductivity atomic force microscopy (LC-AFM) was used for mapping of surface electrical conductivity, and XPS (using AXIS SUPRA (Kratos)) was used for chemical analysis. Before the measurements, the graphene/Ge(001) samples were annealed at 600 K for 30 min in UHV in order to remove physisorbates. STM images visualized by the WSxM package [35].

3. Results and discussion

In the first place, we focus on the graphene on top of Ge(001)/Si(001) substrates affected by the exposition to ambient air condition. Fig. 1 presents the AFM topographies of samples exposed to ambient conditions for four different durations: four days, two weeks, three months and finally six months.

It is clearly seen that nanofacets formed during graphene growth were degraded as a result of the long exposure to atmosphere. However, we noticed that the sample exposed only for four days shows no significant visual changes in morphology. The longer the exposition period the higher sample degradation is observed – as seen in Fig. 1 (c) and (d). The samples were also investigated by XPS technique showing no visible sign of oxidation for two weeks of atmosphere exposure (see Fig. S2 in Supplementary Materials) which is in according for pervious findings [28]. However, the careful analysis of AFM and XPS results leads to the conclusion that the sensitivity of the XPS technique is not sufficient to study early stages of oxidation of the graphene/Ge(001)/Si(001) sample. Therefore, we have to apply a technique which gives us better spatial resolution together with spectroscopic capabilities aiming to resolve oxidized stages, if they exist. In order to do so, we applied KPFM to investigate local contact potential differences (CPD) of graphene/Ge(001)/Si(001) exposed to ambient condition for two weeks. The experiments were performed both under ambient (Fig. 2(a,b)) and in UHV conditions (Fig. 2(c,d)). In the topography image (Fig. 2(a)), we can easily identify regions with distorted nanofacet structure.

They are accompanied with substantial changes of the CPD signal – blue regions in Fig. 2(b). We would like to mention that before the KPFM measurements on the graphene/Ge(001)/Si(001) sample the CPD signal was calibrated with respect to the pure graphene layer. According to this calibration, the yellow color is attributed to CPD signal typical for pure graphene. The dark blue and blue colors are ascribed to the material having a different work function in comparison with graphene. The observed distortion/CPD changes might be related to the presence of either contamination or oxidation, or both. In order to exclude the presence of surface contamination, our sample was heated at 600 K in UHV condition for 1 h before the KPFM measurements depicted in Fig. 2(c)(d). The topography images still show the presence of

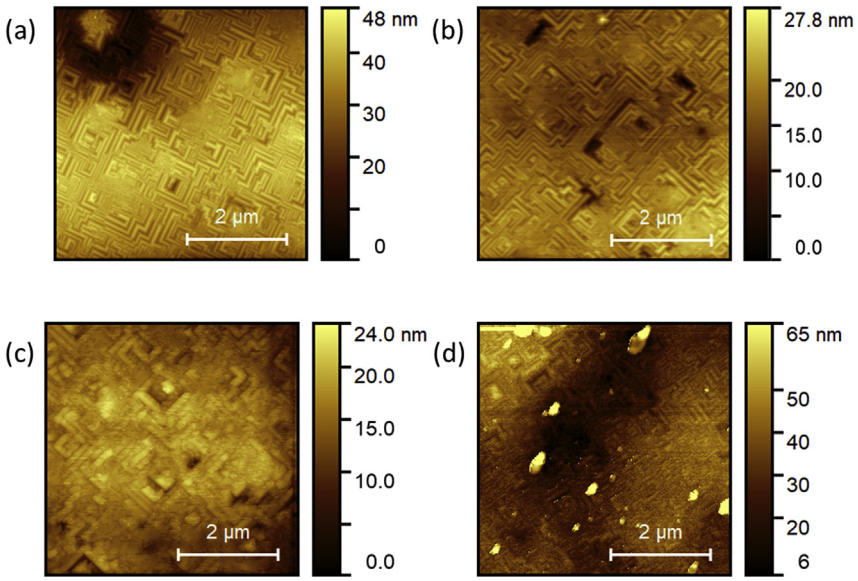

Fig. 1. AFM results of graphene/Ge(001)/Si(001) samples recorded after exposition to ambient condition for (a) four days, (b) two weeks, (c) three months and (d) six months. (A colour version of this figure can be viewed online.)

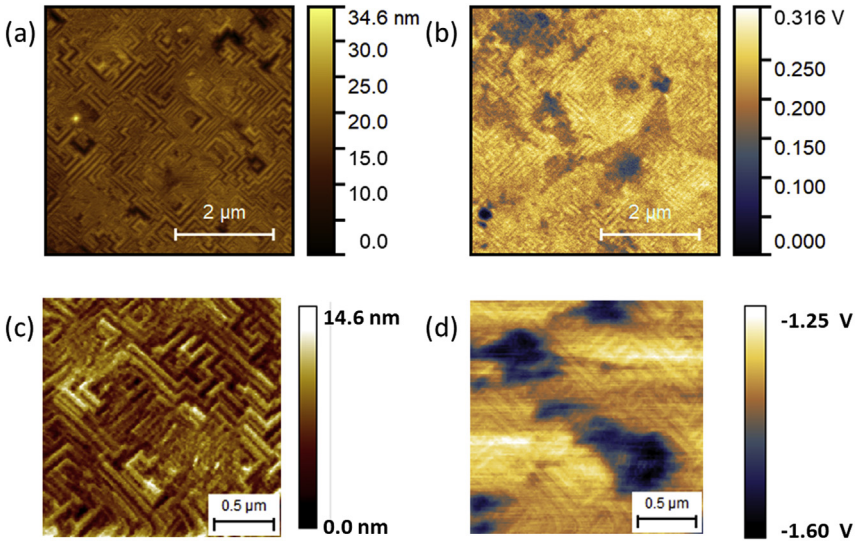

Fig. 2. KPFM results recorded on graphene/Ge(001)/Si(001) sample exposed to ambient condition for two weeks. (a), (b) AFM topography and corresponding CPD map recorded in ambient condition. (c), (d) AFM topography and corresponding CPD map recorded in UHV condition after sample heating at 600 K for 1 h. (A colour version of this figure can be viewed online.)

distorted nanofacets, which can be correlated with the high CPD signal changes (blue spots in the image). It should be emphasized that CPD values and topographic contrast differ from those observed in atmospheric conditions. The observed changes are caused by the use of different tips as well as humidity and surface contaminations when measurements are performed in ambient. Therefore, in order to precisely measure work function, all the experiments should be carried out on clean and conducting samples under UHV condition [36].

In order to make valuable conclusions whether we are dealing with oxidized regions on the graphene/Ge(001)/Si(001) sample or not, the KPFM measurements were performed on the graphene/Ge(001)/Si(001) sample subjected to oxygen exposure during the growth process, which is a reference sample for our analysis.

The topography measurements of the sample subjected to oxygen exposure during the growth (Fig. 3(a) and (c)) clearly show changes identified as circular objects with height close to 30 nm. This is in contradiction to the graphene/Ge(001)/Si(001) sample exposed to ambient condition for two weeks revealing distorted nanofacet structure only (Fig. 2(a),(b)). In KPFM CPD maps presented in Fig. 3 (b) and (d) the yellow regions have high CPD values resulting from complete oxidation processes and can be ascribed to the presence of non-conducting circular objects visible on the topography (Fig. 3(a) and (c)). The non-conducting character of these regions is confirmed by LC-AFM investigations as presented in Fig. 4, which also proves that they are not covered by graphene.

Furthermore, we would like to emphasize that yellow CPD contrast comes from the convolution of topography and electrostatic interactions. Thus, special care must be taken when CPD maps are analyzed. In this place we would like to underline that the

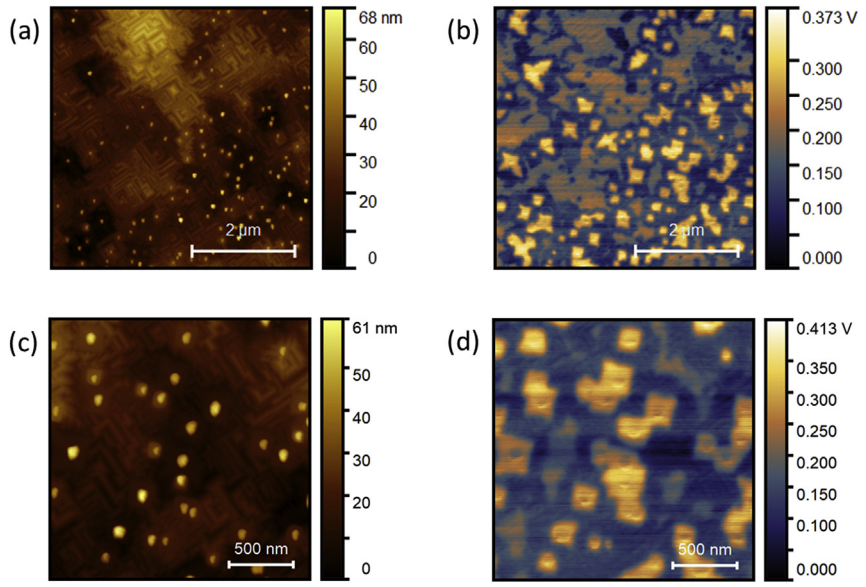

Fig. 3. KPFM results recorded on graphene/Ge(001)/Si(001) sample subjected to oxygen during the growth process and treated as a reference sample. (a,c) KPFM topographies, (b,d) CPD maps. (A colour version of this figure can be viewed online.)

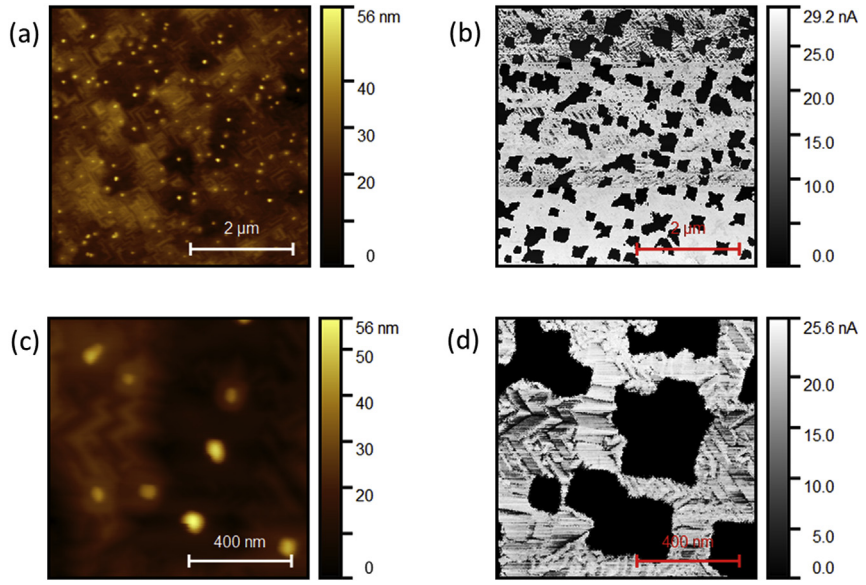

Fig. 4. LC-AFM results recorded on graphene/Ge(001)/Si(001) sample subjected to oxygen exposure during the growth process.(a,c) sample topographies, (b,d) local current maps (dark regions indicate the lack of electrical conductivity). (A colour version of this figure can be viewed online.)

relative CPD values (between dark yellow and dark blue) measured for graphene regions on the reference sample (Fig. 3(b),(d)) are similar to CPD values recorded for the yellow regions visible for the sample exposed to atmospheric conditions for two weeks (Fig. 2). It means that those regions should be ascribed to the presence of pure graphene/germanium interface. Following this convention the blue regions correspond to early oxidation stages as is in the case of graphene/Ge(001)/Si(001) sample after 2 weeks of atmospheric exposure (Fig. 2(b)).

The results show that the distortion of the topography and changes of the CPD signal can be ascribed to the presence of oxidized regions on the surface. Based on these results we attribute the contrast in CPD map presented in Fig. 2 to the presence of the early stages of germanium oxidation. Moreover, we noticed that the oxidation can take place also under graphene. This is well visible in Fig. 5(a), where high resolution topographic AFM over the nanofacets was achieved – see regions 1 denoted by white contours.

Particularly, in the region 1 very sharp edges of the nanofacets are visible. The CPD signal recorded over this region (Fig. 5(b),(c)) is typical for pure graphene, which means that no germanium oxidation processes took place. However, the edges of the nanofacets seem to be slightly smeared when the region 2 is considered. It might be attributed to the very early stages of germanium oxidation beneath the graphene layer. This assumption is confirmed by the CPD map which shows that in the region 2 the germanium substrate is oxidized and at the same time the region is still covered with graphene. The last is proved by the presence of the nanofacets and by the further investigation with scanning

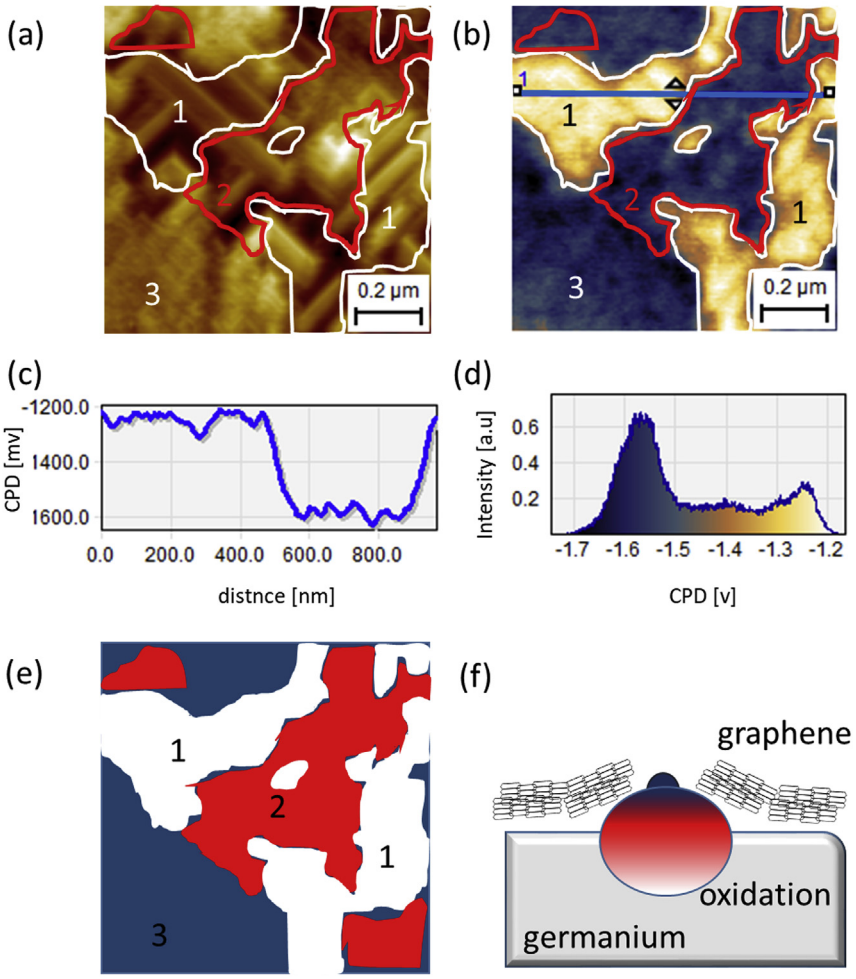

Fig. 5. KPFM results recorded on graphene/Ge(001)/Si(001) sample exposed to ambient condition for two weeks. (a) topography, (b) CPD map, (c) CPD profile along blue line in (b), (d) CPD distribution (e) and (f) scheme of the oxidation process penetration underneath the graphene layer. (A colour version of this figure can be viewed online.)

tunneling spectroscopy presented in Fig. 6. It is reasonable to assume that oxidation of germanium substrate starts from the point where discontinuity of the graphene layers takes place (as region 3 presented in Fig. 5(a)) and penetrates substrate under graphene.

The schematic presentation of the described oxidation process is shown in Fig. 5 (e),(f). The discontinuities in graphene layers were formed during graphene layers growth due to domains misalignment [15,37] Those discontinuities act as a starting point for oxidation process which was marked as a dark filament in Fig. 5 (f) and which corresponds with region 3 in Fig. 5 (e). It has been known that germanium oxides are unstable [30,31] and due to this fact we can observe penetration of the oxidation process under graphene. The results of such process are visible in region 2 in Fig. 5(e). What is more during oxidation, surface roughness increases and continuity of graphene layers is destroyed (Fig. 5(f)), which increases the rate of the oxidation process. Due to instability of the germanium oxides, graphene was fragmented and detached from surface (as in region 3). Finally this process causes degradation of the whole germanium substrate during sufficient timeline, which is visible on Fig. 1(d).

In this place, we also would like to emphasize that the early stages of oxidation were not identified by XPS technique [28], which proved the advantage of the KPFM technique in our studies. Particularly, the CPD map (Fig. 5(b)) together with CPD distribution curve (Fig. 5(c)) can be treated as the equivalent of chemical distribution maps typical for XPS technique, but with significantly higher sensitivity and spatial resolution.

Since the CPD signal is directly related to the electronic structure of the surface, it is useful to correlate the KPFM data with the scanning tunneling spectroscopy results. This is because the STS data gives direct information about electron local density of states (LDOS) of the sample surface [38]. Typical STM topography and LDOS profile of the unaffected graphene/Ge(001)/Si(001) sample is shown as a reference in Supplementary Materials – Fig. S3. The STM topography of the graphene/Ge(001)/Si(001) sample exposed to atmospheric environment for two weeks is presented in Fig. 6(a).

It shows blurry distorted nanofacets caused by the oxidation processes. We also show LDOS (in Figs. 6(b) and 4(c)) maps correlated with the STM topography, which were recorded at energies +0.3 eV and −0.3 eV from the Fermi level. On the LDOS maps the dark blue color corresponds to low value of LDOS, while the green/red color corresponds to high value of LDOS. The visible heterogeneity of electronic structure might be caused by the presence of surface defects or regions in which coexistence of different oxidation stages took place.

Comparing STM topography with the LDOS maps we conclude that the more distorted regions of the graphene/Ge(001)/Si(001) sample the lower value of LDOS. It means that in these regions we are dealing with semiconducting properties of the surface. Particularly, this is well visible when we compare a LDOS profile recorded

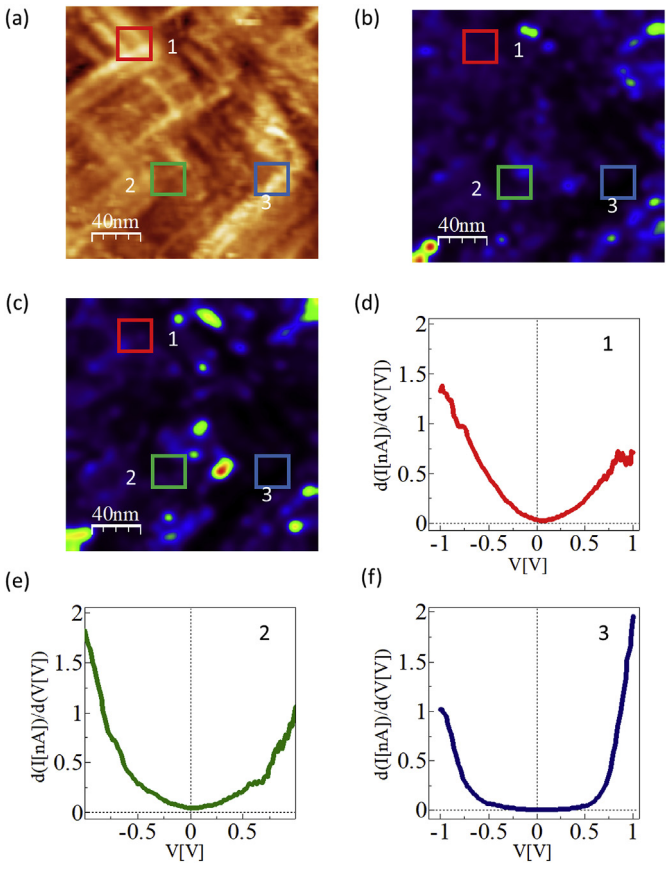

Fig. 6. STM/STS/CITS results for the graphene/Ge(001)/Si(001) sample. (a) STM topography. (b),(c) LDOS maps recorded at −0.3 eV and 0.3 eV relative to the Fermi level and correlated with STM topography shown in (a). On the LDOS maps the dark blue color corresponds to low value of LDOS, while the green/red color corresponds to high value of LDOS. (d),(e) and (f) show dI/dV curves recorded in regions marked as #1, #2 and #3, respectively. (A colour version of this figure can be viewed online.)

in undistorted region #1 (presented in Fig. 6(d)), with those from region #2 and #3 (presented in Fig. 6(e) and (f)) recorded on somewhat distorted sample surface. In regions #2 and #3 the semiconducting properties occurred, although Ge(001) terraces should promote the growth of high-quality graphene [20,23,37] and on the top of the nanofacets the semimetalic like spectra should be observed (as it is for region #1 and for high quality graphene presented in Fig. S3 in Supplementary Materials). The LDOS profile recorded on regions #3 (Fig. 6(f)) shows a distinct energy gap, which can be ascribed to the presence of germanium oxides on the surface. Additionally on those regions there were no signs observed from graphene during STM measurements in atomic resolution mode which is not the case for region 1 and 2. It is worth to emphasize that LDOS profiles measured in the region #2 which is placed somewhat between undistorted and distorted nanofacets also show substantial deviation from the typical graphene LDOS shape. In these regions, the measured dI/dV curves have quadratic behavior (Fig. 6(e)), which indicates a strong interaction between graphene and substrate probably due to the oxidation processes, which penetrated under the graphene layer. The appearance of these interactions can also generate significant strength in the graphene layer and finally can lead to appearance of the cracks between graphene domains. This is important when graphene is transferred from germanium onto other substrates. Finally, it is worth emphasizing that the STM/STS/CITS results can be directly correlated with the KPFM data. In both techniques, the topography images showed distorted nanofacets structures ascribed to the germanium oxidized regions. It is worth pointing out that KPFM measurements were significantly less time consuming than STM/STS, and additionally they could be performed for devices where some part of the samples were not conducting without causing any particular damage of tip and sample.

4. Conclusions

The KPFM and STM/STS techniques were used to study early stages of oxidation of germanium in the graphene/Ge(001)/Si(001) system exposed to atmospheric environment. It was found that in CVD process always some discontinuities in graphene layer appear as a result of graphene multi-domain formation of different orientations with respect to the Ge(001) substrate. These discontinuities are origin of oxidation sites, from which oxidation propagate underneath the graphene layer. This takes place in a similar way as in the previously studied graphene on copper system. Since germanium substrate is more reactive than copper, corrosion processes are much faster, even in the case of a smaller number of planar graphene domain orientations. This means that single-layer graphene is insufficient to protect germanium substrate in a long time scale. However, it should be emphasized that even a few days of exposure to ambient conditions can cause only nanoscale oxidation processes of germanium. It gives sufficient time to manufacture a graphene device or to transfer graphene onto another substrate but more graphene layers or encapsulation process should be performed to avoid device degradation in a long time scale. We have also proven that KPFM can be efficiently used to assess the quality of graphene produced on substrates compatible with CMOS technology. Moreover, we showed that XPS were insufficient to study early stages of oxidation of the germanium substrate.

Acknowledgments

The research leading to these results was financially supported by the National Science Centre, Poland, Grants No. 2015/19/D/ST5/01933, 2016/23/D/ST5/00633 and 2016/21/B/ST5/00984. M.R. was supported by the University of Lodz (Grant supporting young scientists). This work was also supported by the EU Graphene Flagship Core 2 (Grant Agreement No. 785219).

Appendix A. Supplementary data

Supplementary data to this article can be found online at https://doi.org/10.1016/j.carbon.2019.04.036.

References

[1] M. Yi, Z. Shen, A review on mechanical exfoliation for the scalable production of graphene, J. Mater. Chem. A. 3 (2015) 11700–11715, https://doi.org/10.1039/C5TA00252D.
[2] S. Pei, H.-M. Cheng, The reduction of graphene oxide, Carbon 50 (2012) 3210–3228, https://doi.org/10.1016/j.carbon.2011.11.010.
[3] W. Norimatsu, M. Kusunoki, Epitaxial graphene on SiC{0001}: advances and perspectives, Phys. Chem. Chem. Phys. 16 (2014) 3501–3511, https://doi.org/10.1039/C3CP54523G.
[4] W. Strupinski, K. Grodecki, A. Wysmolek, R. Stepniewski, T. Szkopek, P.E. Gaskell, A. Grüneis, D. Haberer, R. Bozek, J. Krupka, J.M. Baranowski, Graphene epitaxy by chemical vapor deposition on SiC, Nano Lett. 11 (2011) 1786–1791, https://doi.org/10.1021/nl200390e.
[5] M. Batzill, The surface science of graphene: metal interfaces, CVD synthesis, nanoribbons, chemical modifications, and defects, Surf. Sci. Rep. 67 (2012) 83–115, https://doi.org/10.1016/j.surfrep.2011.12.001.
[6] M.H. O Jr., T. Schumann, F. Fromm, R. Koch, M. Ostler, M. Ramsteiner, T. Seyller, J.M.J. Lopes, H. Riechert, Formation of high-quality quasi-free-standing bilayer graphene on SiC(0 0 0 1) by oxygen intercalation upon annealing in air, Carbon 52 (2013) 83–89, https://doi.org/10.1016/

j.carbon.2012.09.008.
[7] C. Riedl, C. Coletti, T. Iwasaki, A.A. Zakharov, U. Starke, Quasi-free-Standing epitaxial graphene on SiC obtained by hydrogen intercalation, Phys. Rev. Lett. 103 (2009) 246804, https://doi.org/10.1103/PhysRevLett.103.246804.
[8] P. Dabrowski, M. Rogala, I. Wlasny, Z. Klusek, M. Kopciuszynski, M. Jalochowski, W. Strupinski, J.M. Baranowski, Nitrogen doped epitaxial graphene on 4H-SiC(0001) – experimental and theoretical study, Carbon 94 (2015) 214–223, https://doi.org/10.1016/j.carbon.2015.06.073.
[9] E. Velez-Fort, C. Mathieu, E. Pallecchi, M. Pigneur, M.G. Silly, R. Belkhou, M. Marangolo, A. Shukla, F. Sirotti, A. Ouerghi, Epitaxial graphene on 4H-SiC(0001) grown under nitrogen flux: evidence of low nitrogen doping and high charge transfer, ACS Nano 6 (2012) 10893–10900, https://doi.org/10.1021/nn304315z.
[10] A. Ambrosi, M. Pumera, The CVD graphene transfer procedure introduces metallic impurities which alter the graphene electrochemical properties, Nanoscale 6 (2014) 472–476, https://doi.org/10.1039/C3NR05230C.
[11] T. Hallam, N.C. Berner, C. Yim, G.S. Duesberg, Strain, bubbles, dirt, and folds: a study of graphene polymer-assisted transfer, Adv. Mater. Interfaces. 1 (2014) 1400115, https://doi.org/10.1002/admi.201400115.
[12] Y.G. Lee, C.G. Kang, U.J. Jung, J.J. Kim, H.J. Hwang, H.-J. Chung, S. Seo, R. Choi, B.H. Lee, Fast transient charging at the graphene/SiO2 interface causing hysteretic device characteristics, Appl. Phys. Lett. 98 (2011) 183508, https://doi.org/10.1063/1.3588033.
[13] L. Di Gaspare, A.M. Scaparro, M. Fanfoni, L. Fazi, A. Sgarlata, A. Notargiacomo, V. Miseikis, C. Coletti, M. De Seta, Early stage of CVD graphene synthesis on Ge(001) substrate, Carbon 134 (2018) 183–188, https://doi.org/10.1016/j.carbon.2018.03.092.
[14] J. Dai, D. Wang, M. Zhang, T. Niu, A. Li, M. Ye, S. Qiao, G. Ding, X. Xie, Y. Wang, P.K. Chu, Q. Yuan, Z. Di, X. Wang, F. Ding, B.I. Yakobson, How graphene islands are unidirectionally aligned on the Ge(110) surface, Nano Lett. 16 (2016) 3160–3165, https://doi.org/10.1021/acs.nanolett.6b00486.
[15] J. Dabrowski, G. Lippert, J. Avila, J. Baringhaus, I. Colambo, Y.S. Dedkov, F. Herziger, G. Lupina, J. Maultzsch, T. Schaffus, T. Schroeder, M. Kot, C. Tegenkamp, D. Vignaud, M.-C. Asensio, Understanding the growth mechanism of graphene on Ge/Si(001) surfaces, Sci. Rep. 6 (2016) 31639, https://doi.org/10.1038/srep31639.
[16] G. Wang, M. Zhang, Y. Zhu, G. Ding, D. Jiang, Q. Guo, S. Liu, X. Xie, P.K. Chu, Z. Di, X. Wang, Direct growth of graphene film on germanium substrate, Sci. Rep. 3 (2013) 2465, https://doi.org/10.1038/srep02465.
[17] J.-H. Lee, E.K. Lee, W.-J. Joo, Y. Jang, B.-S. Kim, J.Y. Lim, S.-H. Choi, S.J. Ahn, J.R. Ahn, M.-H. Park, C.-W. Yang, B.L. Choi, S.-W. Hwang, D. Whang, Wafer-scale growth of single-crystal monolayer graphene on reusable hydrogen-terminated germanium, Science 344 (80) (2014) 286–289, https://doi.org/10.1126/science.1252268.
[18] G. Lippert, J. Dąbrowski, T. Schroeder, M.A. Schubert, Y. Yamamoto, F. Herziger, J. Maultzsch, J. Baringhaus, C. Tegenkamp, M.C. Asensio, J. Avila, G. Lupina, Graphene grown on Ge(0 0 1) from atomic source, Carbon 75 (2014) 104–112, https://doi.org/10.1016/j.carbon.2014.03.042.
[19] I. Pasternak, M. Wesolowski, I. Jozwik, M. Lukosius, G. Lupina, P. Dabrowski, J.M. Baranowski, W. Strupinski, Graphene growth on Ge(100)/Si(100) substrates by CVD method, Sci. Rep. 6 (2016) 21773. https://doi.org/10.1038/srep21773.
[20] R.M. Jacobberger, B. Kiraly, M. Fortin-Deschenes, P.L. Levesque, K.M. McElhinny, G.J. Brady, R. Rojas Delgado, S. Singha Roy, A. Mannix, M.G. Lagally, P.G. Evans, P. Desjardins, R. Martel, M.C. Hersam, N.P. Guisinger, M.S. Arnold, Direct oriented growth of armchair graphene nanoribbons on germanium, Nat. Commun. 6 (2015) 8006, https://doi.org/10.1038/ncomms9006.
[21] B. Kiraly, R.M. Jacobberger, A.J. Mannix, G.P. Campbell, M.J. Bedzyk, M.S. Arnold, M.C. Hersam, N.P. Guisinger, Electronic and mechanical properties of graphene–germanium interfaces grown by chemical vapor deposition, Nano Lett. 15 (2015) 7414–7420, https://doi.org/10.1021/acs.nanolett.5b02833.
[22] J. Grzonka, I. Pasternak, P.P. Michałowski, V. Kolkovsky, W. Strupinski, Influence of hydrogen intercalation on graphene/Ge(0 0 1)/Si(0 0 1) interface, Appl. Surf. Sci. 447 (2018) 582–586, https://doi.org/10.1016/j.apsusc.2018.04.029.
[23] I. Pasternak, P. Dabrowski, P. Ciepielewski, V. Kolkovsky, Z. Klusek, J.M. Baranowski, W. Strupinski, Large-area high-quality graphene on Ge(001)/Si(001) substrates, Nanoscale 8 (2016) 11241–11247, https://doi.org/10.1039/C6NR01329E.
[24] I. Wlasny, P. Dabrowski, M. Rogala, I. Pasternak, W. Strupinski, J.M. Baranowski, Z. Klusek, Impact of electrolyte intercalation on the corrosion of graphene-coated copper, Corros. Sci. 92 (2015) 69–75, https://doi.org/10.1016/j.corsci.2014.11.027.
[25] M. Schriver, W. Regan, W.J. Gannett, A.M. Zaniewski, M.F. Crommie, A. Zettl, Graphene as a long-term metal oxidation barrier: worse than nothing, ACS Nano 7 (2013) 5763–5768, https://doi.org/10.1021/nn4014356.
[26] D. Prasai, J.C. Tuberquia, R.R. Harl, G.K. Jennings, K.I. Bolotin, Graphene: corrosion-inhibiting coating, ACS Nano 6 (2012) 1102–1108, https://doi.org/10.1021/nn203507y.
[27] I. Wlasny, P. Dabrowski, M. Rogala, P.J. Kowalczyk, I. Pasternak, W. Strupinski, J.M. Baranowski, Z. Klusek, Role of graphene defects in corrosion of graphene-coated Cu(111) surface, Appl. Phys. Lett. 102 (2013), https://doi.org/10.1063/1.4795861.
[28] R. Rojas Delgado, R.M. Jacobberger, S.S. Roy, V.S. Mangu, M.S. Arnold, F. Cavallo, M.G. Lagally, Passivation of germanium by graphene, ACS Appl. Mater. Interfaces 9 (2017) 17629–17636, https://doi.org/10.1021/acsami.7b03889.
[29] F. Yu, L. Camilli, T. Wang, D.M.A. Mackenzie, M. Curioni, R. Akid, P. Bøggild, Complete long-term corrosion protection with chemical vapor deposited graphene, Carbon 132 (2018) 78–84, https://doi.org/10.1016/j.carbon.2018.02.035.
[30] D. Bodlaki, H. Yamamoto, D. Waldeck, E. Borguet, Ambient stability of chemically passivated germanium interfaces, Surf. Sci. 543 (2003) 63–74, https://doi.org/10.1016/S0039-6028(03)00958-0.
[31] D. Schmeisser, R.D. Schnell, A. Bogen, F.J. Himpsel, D. Rieger, G. Landgren, J.F. Morar, Surface oxidation states of germanium, Surf. Sci. 172 (1986) 455–465, https://doi.org/10.1016/0039-6028(86)90767-3.
[32] G.W. Anderson, M.C. Hanf, P.R. Norton, Z.H. Lu, M.J. Graham, The S-passivation of Ge(100)-(1×1), Appl. Phys. Lett. 66 (1995) 1123–1125, https://doi.org/10.1063/1.113833.
[33] T. Deegan, G. Hughes, An X-ray photoelectron spectroscopy study of the HF etching of native oxides on Ge(111) and Ge(100) surfaces, Appl. Surf. Sci. 123–124 (1998) 66–70, https://doi.org/10.1016/S0169-4332(97)00511-4.
[34] K.M. McElhinny, R.M. Jacobberger, A.J. Zaug, M.S. Arnold, P.G. Evans, Graphene-induced Ge (001) surface faceting, Surf. Sci. 647 (2016) 90–95, https://doi.org/10.1016/j.susc.2015.12.035.
[35] I. Horcas, R. Fernández, J.M. Gómez-Rodríguez, J. Colchero, J. Gómez-Herrero, A.M. Baro, WSXM: a software for scanning probe microscopy and a tool for nanotechnology, Rev. Sci. Instrum. 78 (2007), https://doi.org/10.1063/1.2432410, 013705.
[36] W. Melitz, J. Shen, A.C. Kummel, S. Lee, Kelvin probe force microscopy and its application, Surf. Sci. Rep. 66 (2011) 1–27, https://doi.org/10.1016/j.surfrep.2010.10.001.
[37] P. Dabrowski, M. Rogala, I. Pasternak, J. Baranowski, W. Strupinski, M. Kopciuszynski, R. Zdyb, M. Jalochowski, I. Lutsyk, Z. Klusek, The study of the interactions between graphene and Ge(001)/Si(001), Nano Res 10 (2017) 3648–3661, https://doi.org/10.1007/s12274-017-1575-6.
[38] J. Tersoff, D.R. Hamann, Theory and application for the scanning tunneling microscope, Phys. Rev. Lett. 50 (1983) 1998–2001, https://doi.org/10.1103/PhysRevLett.50.1998.